Determination of Hydroperoxyl/superoxide Anion Radical ($HO_2^{\cdot}/O_2^{\cdot-}$) Concentration in the Decomposition of Ozone Using a Kinetic Method

Bum Gun Kwon[a] and Jai H. Lee*

*Department of Environmental Science and Engineering, Gwangju Institute of Science and Technology (GIST), Gwangju 500-712, Korea. *E-mail: jhlee@gist.ac.kr*

Received June 3, 2006

A novel kinetic method for determination of $HO_2^{\cdot}/O_2^{\cdot-}$ in ozone decomposition in water is described. In this study, potential interferences of O_3 and the hydroxyl radicals, $^{\cdot}OH_{(O3)}$, are suppressed by HSO_3^-/SO_3^{2-}. $HO_2^{\cdot}/O_2^{\cdot-}$ formed in ozone decomposition reduces Fe^{3+}-EDTA into Fe^{2+}-EDTA and subsequently the well-known Fenton-like (FL) reaction of H_2O_2 and Fe^{2+}-EDTA produces the hydroxyl radicals, $^{\cdot}OH_{(FL)}$. Benzoic acid (BA) scavenges $^{\cdot}OH_{(FL)}$ to produce OHBA, which are analyzed by fluorescence detection (λ_{ex} = 320 nm and λ_{em} = 400 nm). The concentration of $HO_2^{\cdot}/O_2^{\cdot-}$ in ozone decomposition has been determined by the novel kinetic method using the experimentally determined half-life ($t_{1/2}$). The steady-state concentration of $HO_2^{\cdot}/O_2^{\cdot-}$ is proportional to the O_3 concentration at a given pH. However, the steady-state concentration of $HO_2^{\cdot}/O_2^{\cdot-}$ in ozone decomposition is inversely proportional to pH values. This pH dependence is due to significant loss of $O_2^{\cdot-}$ by O_3 at higher pH conditions. The steady-state concentrations of $HO_2^{\cdot}/O_2^{\cdot-}$ are in the range of $2.49\ (\pm 0.10) \times 10^{-9}$ M (pH = 4.17) ~ $3.01\ (\pm 0.07) \times 10^{-10}$ M (pH = 7.59) at $[O_3]_o$ = 60 μM.

Key Words : Hydroperoxyl radical, Superoxide anion radical, Ozone, Fenton-like, Hydroxyl radical

Introduction

The chemistry of ozone is of major interest in drinking water and wastewater treatment processes since ozone has been recognized as a potent oxidant to improve taste, color, disinfection, and degradation of pollutants.[1] During ozone decomposition in water, however, the two major oxidants, ozone and the hydroxyl radicals ($^{\cdot}OH_{(O3)}$), govern the oxidative processes.[2-7] The reaction of transient hydroperoxyl/superoxide anion radical ($HO_2^{\cdot}/O_2^{\cdot-}$) with ozone is one of the possible formation pathways for generating $^{\cdot}OH_{(O3)}$. This reaction has found comparable interest considering the production of the highly reactive $^{\cdot}OH_{(O3)}$ to eliminate ozone-refractory compounds in water treatment processes.[8]

Numerous studies on the $HO_2^{\cdot}/O_2^{\cdot-}$ reactions in the decomposition of aqueous ozone are now available in several studies.[2-7,9,10] So far, the best reaction model to explain the decomposition of ozone in water is the chain mechanism suggested by the elegant works of Hoigne and co-workers as follow:[1,8]

$$O_3 + OH^- \rightarrow HO_2^- + O_2 \quad (1)$$
$$HO_2^- + H^+ \leftrightarrow H_2O_2 \quad pK_a = 11.6 \quad (2)$$
$$HO_2^- + O_3 \rightarrow O_2^{\cdot-} + {}^{\cdot}OH_{(O3)} + O_2 \quad (3)$$
$$H_2O_2 + O_3 \rightarrow HO_2^{\cdot} + {}^{\cdot}OH_{(O3)} + O_2 \quad (4)$$
$$O_2^{\cdot-} + H^+ \leftrightarrow HO_2^{\cdot} \quad pK_a = 4.8 \quad (5)$$
$$O_2^{\cdot-} + O_3 \rightarrow O_2 + O_3^{\cdot-} \quad (6)$$
$$HO_2^{\cdot} + O_3 \rightarrow 2O_2 + {}^{\cdot}OH_{(O3)} \quad (7)$$
$$O_3^{\cdot-} \rightarrow O_2 + O^{\cdot-} \quad (8)$$
$$O^{\cdot-} + H^+ \leftrightarrow {}^{\cdot}OH_{(O3)} \quad pK_a = 11.8 \quad (9)$$
$$^{\cdot}OH_{(O3)} + O_3 \rightarrow HO_2^{\cdot} + O_2 \quad (10)$$
$$^{\cdot}OH_{(O3)} + \text{Pollutants} \rightarrow \text{Products} \quad (11)$$

In aqueous solution of ozone, the initiation of ozone decomposition can be accelerated with increasing the concentration of hydroxide ion, and ozone decomposition is propagated by hydrogen peroxide (H_2O_2/HO_2^-). The reaction between O_3 and H_2O_2/HO_2^- leads to the formation of $^{\cdot}OH_{(O3)}$, $HO_2^{\cdot}$, and O_2. Subsequently, $O_2^{\cdot-}$ reacts with O_3 to produce $O_3^{\cdot-}$, which is decomposed to O_2 and $O^{\cdot-}$. The additional hydroxyl radicals, $^{\cdot}OH_{(O3)}$, is generated in an acid-base equilibrium of $O^{\cdot-}$ (reactions 7-9). Then $^{\cdot}OH_{(O3)}$ reacts rapidly with O_3 producing $HO_2^{\cdot}$. Thus, the decomposition of O_3 is accelerated by radical-type chain reactions. However, ozone-refractory compounds in reaction 11 may compete with O_3 for $^{\cdot}OH_{(O3)}$.

Up to now, two methods have been available for the detection and/or determination of $HO_2^{\cdot}/O_2^{\cdot-}$ in ozone decomposition reactions: a) the kinetic spectroscopy in pulse radiolysis of aqueous ozone solutions;[2,11] b) the reduction of tetranitromethane (TNM, $C(NO_2)_4$) as an $HO_2^{\cdot}/O_2^{\cdot-}$ indicator.[6,8] In the kinetic spectroscopy method, both $HO_2^{\cdot}$ and $O_2^{\cdot-}$ formed in the decomposition of electron-irradiated aqueous ozone have distinct absorption spectra ($\varepsilon_{HO_2^{\cdot}}^{220nm} \approx 1{,}350\ M^{-1}cm^{-1}$ and $\varepsilon_{O_2^{\cdot-}}^{220nm} \approx 1{,}900\ M^{-1}cm^{-1}$) at pH 2 and 10.5, respectively.[9,11] This method, however, has been limited in O_3 solution by the spectrum overlapping since many chemical species, *i.e.*, $^{\cdot}OH$ ($\varepsilon_{220nm} \approx 550\ M^{-1}cm^{-1}$)[11] and O_3 ($\varepsilon_{220nm} = 516\ M^{-1}cm^{-1}$ as estimated value) (see Appendix), absorb strongly at wavelength 220 nm. The use of the kinetic spectroscopy has only focused on the rate constant data of $HO_2^{\cdot}/O_2^{\cdot-}$ with ozone.[2,11] In the TNM method, the reaction of TNM with $HO_2^{\cdot}/O_2^{\cdot-}$ at diffusion-controlled rate ($k = 2 \times 10^9\ M^{-1}s^{-1}$) produces the nitroform

[a]Present address: Environmental & Whole Information System (E&WIS), Seoul 151-848, Korea.

anion, $C(NO_2)_3^-$ (NF^-) with intense optical absorbance (ε_{350nm} = 15,000 $M^{-1}cm^{-1}$).[8] However, the spectrophotometric method using TNM has suffered from low sensitivity,[12] and a consumption of NF^- by ozone as well as a rapid production of NF^- by the hydrolysis of TNM has to be taken into account.[8] This method has high uncertainty for the quantitative determination of $HO_2^{\cdot}/O_2^{\cdot-}$ concentration. Nevertheless, information on the concentration of $HO_2^{\cdot}/O_2^{\cdot-}$ has been so far limited in earlier studies involving O_3 chemistry in aqueous solution.

For an alternative method of determining the $HO_2^{\cdot}/O_2^{\cdot-}$, Kwon *et al.*[12] developed a new kinetic method as an analytical tool for the measurement of $HO_2^{\cdot}/O_2^{\cdot-}$ in aqueous solution. This new method is based on the reduction of Fe^{3+}-EDTA into Fe^{2+}-EDTA by $HO_2^{\cdot}/O_2^{\cdot-}$ and the subsequent well-known Fenton-like (FL) reaction of H_2O_2 and Fe^{2+}-EDTA to yield the hydroxyl radicals, $^{\cdot}OH_{(FL)}$. Benzoic acid (BA) scavenges $^{\cdot}OH_{(FL)}$ to produce hydroxybenzoic acids (OHBA), which are analyzed by fluorescence detection (λ_{ex} = 320 nm and λ_{em} = 400 nm). The concentration of $HO_2^{\cdot}/O_2^{\cdot-}$ in ozone decomposition has been determined by the novel kinetic method using the experimentally determined half-life ($t_{1/2}$). The new kinetic method has shown high sensitivity and simple calibration system. It can contribute significantly to the studies of $HO_2^{\cdot}/O_2^{\cdot-}$ at very low concentrations as well as of the basic function of $HO_2^{\cdot}/O_2^{\cdot-}$.

In this study, the optimization of the kinetic method in aqueous ozone decomposition and the quantitative determination of $HO_2^{\cdot}/O_2^{\cdot-}$ concentration are investigated. The reactions of O_3 with H_2O_2/HO_2^- and $HO_2^{\cdot}/O_2^{\cdot-}$ produce the hydroxyl radicals, $^{\cdot}OH_{(O3)}$, through reactions of 3-4 and 8-9, which may interfere with the additional formation of OHBA. In addition, the OHBA formation may be resulted from the direct oxidative reaction of O_3 with BA:[5]

$$O_3 + BA \rightarrow\rightarrow\rightarrow OHBA \qquad (12)$$

Hence potential OHBA formation by reactions of O_3 and $^{\cdot}OH_{(O3)}$ with BA should be effectively suppressed, which was performed by addition of HSO_3^-/SO_3^{2-} depending on the ozone solution pH.

Experimental Section

Materials. Ozone is generated with a dioxygen (purity, 99.99%)-fed ozone generator (Ozonia Triogen, model LAB2A). The aqueous stock solution of ozone is generated with bubbling the gas-phase ozone through a gas-washing bottle (500 mL) filled with slightly acidic deionized water. The concentration of aqueous ozone stock solution is determined spectrophotometrically by measuring the absorbance at 258 nm (ε = 2,900 $M^{-1}cm^{-1}$).[13] Stock solution is then pipetted into a reaction flask where it is diluted in proper level with buffer solution. The solution pH is adjusted to the ranges between 4 and 10 with phosphate buffer (Sigma) and borate buffer (LabChem Inc.) along with H_2SO_4 and NaOH. Potential OHBA formation reactions by

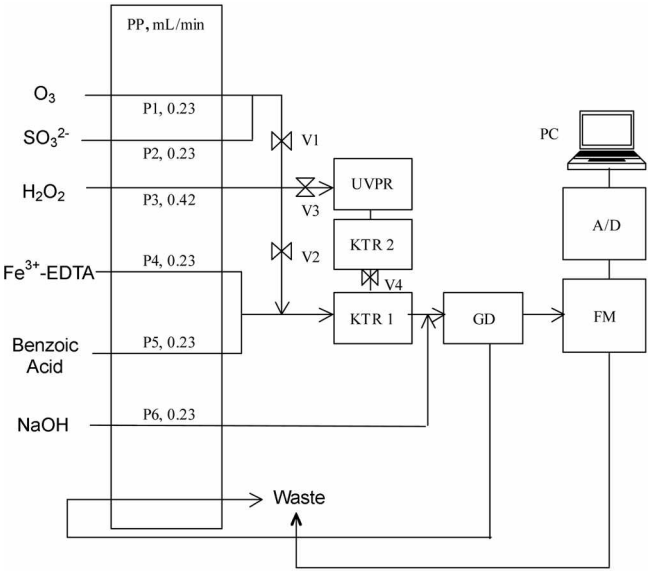

Figure 1. Schematic diagram and calibration equipment for measuring $HO_2^{\cdot}/O_2^{\cdot-}$. PP, peristaltic pump; UVPR, UV photolysis reactor; KTR1, KTR2, knotted tubing reactors; GD, glass debubbler; FM, fluorometer; A/D, A/D converter; PC, computer; P1, P2, P3, P4, P5, P6, and P7, solution inlet ports; V1, V2, V3, and V4, manually operated valves.

O_3 and $^{\cdot}OH_{(O3)}$ with BA are quenched with Na_2SO_3 (Sigma). Ferric ethylenediaminetetra acetate (Fe^{3+}-EDTA), ferrous sulfate, ferric sulfate, sulfuric acid, sodium hydroxide, benzoic acid (BA), and 3% hydrogen peroxide are of reagent grade, and are purchased from Sigma-Aldrich. The concentration of the stock H_2O_2 solution is determined by using $KMnO_4$ titration method prior to use. Working solution of H_2O_2 is prepared daily by diluting the H_2O_2 stock in proper level with high-purity deionized water. The standard $HO_2^{\cdot}/O_2^{\cdot-}$ solution is prepared by the photolysis of H_2O_2 solution at wavelength 254 nm.[12] All solutions are made with high-purity water from Millipore ultra-purification system (> 18 MΩ cm).

$HO_2^{\cdot}/O_2^{\cdot-}$ measurement system in ozone process. A schematic diagram for $HO_2^{\cdot}/O_2^{\cdot-}$ measurement is shown in Figure 1. The apparatus and the experimental procedures employed in the present study are similar to a previous study[12] except for the HSO_3^-/SO_3^{2-} and O_3 ports. All solutions are delivered by using peristaltic pump (Ismatec) with PTFE tubing (Cole-Parmer, i.d. 0.8 mm).

During measurement of $HO_2^{\cdot}/O_2^{\cdot-}$, V1 (valve 1) and V2 (valve 2) are opened, while V3 and V4 are closed, and O_3 solution is delivered through the port 1 (P1, 0.23 mL/min). The OH^--initiated decomposition of O_3 leads to the formation of $HO_2^{\cdot}/O_2^{\cdot-}$, $^{\cdot}OH_{(O3)}$, and O_2.[2] Solution of SO_3^{2-} is added through the port 2 (P2, 0.23 mL/min) eliminating the residual O_3 and $OH_{(O3)}$ which may react with BA to produce extra OHBA. Excess H_2O_2 in the port 3 (P3, 0.42 mL/min) destroys leftover HSO_3^-/SO_3^{2-} and is mixed with a premixed solution containing Fe^{3+}-EDTA (port 4, 0.23 mL/min) and BA (port 5, 0.23 mL/min). Fe^{3+}-EDTA is reduced by $O_2^{\cdot-}$ to Fe^{2+}-EDTA with $k_{13} = 2 \times 10^6$ M^{-1} s^{-1}:[9]

$$Fe^{3+}\text{-EDTA} + O_2^{\cdot-} \rightarrow Fe^{2+}\text{-EDTA} + O_2 \quad (13)$$

Subsequent Fenton-like reaction between Fe^{2+}-EDTA and H_2O_2 ($k_{14} = (2 \pm 1) \times 10^4\ M^{-1}\ s^{-1}$) leads to the production of $\cdot OH_{(FL)}$ and the regeneration of Fe^{3+}-EDTA:[14]

$$Fe^{2+}\text{-EDTA} + H_2O_2 \rightarrow Fe^{3+}\text{-EDTA} + OH^- + {}^{\cdot}OH_{(FL)} \quad (14)$$

Then, $^{\cdot}OH_{(FL)}$ produces OHBA in the presence of BA with a nearly diffusion-controlled rate constant of $k_{15} = 4.3 \times 10^9\ M^{-1}\ s^{-1}$ in KTR1 (knotted tubing reactor 1):[15]

$$^{\cdot}OH_{(FL)} + BA \rightarrow OHBA \quad (15)$$

After, 0.05 N NaOH through the port 6 (P6, 0.23 mL/min) is added to raise pH level above 11 at which the fluorescence signal of OHBA can be maintained at a maximum level. The mixed solution occasionally causes the formation of air bubble in the effluent stream, which is removed by a glass debubbler (GD) prior to the fluorometer (FM) in order to prevent a noise signal by the air bubbles.

The OHBA fluorescence is then measured with a fluorometer (Waters 474 model) equipped with a 16 μL flow-through cell using λ_{ex} = 320 nm / λ_{em} = 400 nm with slit-width of 40 nm. The fluorescence signal is transferred to a data acquisition system, *Auto-chrowin* (Younglin, Korea), consisting of an analog-to-digital converter (A/D) with a personal computer (PC).

Calibration procedures for $HO_2^{\cdot}/O_2^{\cdot-}$. The calibration employed in this work is described in detail in the previous study.[12] Briefly, during calibration of the system, V3 and V4 are opened, while V1 is by-passed and V2 is closed. All working solutions containing 4 mM H_2O_2, 20 μM Fe^{3+}-EDTA, 1 mM benzoic acid (BA), and 0.05 N NaOH are passed through the appropriate ports under UV lamp-off and the base lines are monitored. H_2O_2 solution ($\varepsilon_{254nm} = 19\ M^{-1}\ cm^{-1}$) placed in UV irradiation under lamp-on using a 4W low pressure Hg lamp (λ_{max} = 254 nm, Philips) is photo-decomposed to produce two OH radicals. Most of the OH radicals formed under UV irradiation react with residual H_2O_2 giving $HO_2^{\cdot}$:

$$H_2O_2 + h\nu \rightarrow 2\ {}^{\cdot}OH \quad (16)$$

$$^{\cdot}OH + H_2O_2 \rightarrow HO_2^{\cdot} + H_2O \quad (17)$$

where $k_{17} = 2.7 \times 10^7\ M^{-1}\ s^{-1}$.[9]

In the absence of additives, $HO_2^{\cdot}$ and $O_2^{\cdot-}$ in knotted tubing reactor 2 (KTR2) are disproportionated by self-reactions of 18 and 19 according to the empirically observed pH-dependent rate constant, k_{obs}:[9]

$$HO_2^{\cdot} + HO_2^{\cdot} \rightarrow H_2O_2 + O_2 \quad (18)$$

$$HO_2^{\cdot} + O_2^{\cdot-} \rightarrow HO_2^- + O_2 \quad (19)$$

$$k_{obs} = \{k_{18} + k_{19}(K_{HO_2}/[H^+])\}/(1 + K_{HO_2}/[H^+])^2 \quad (I)$$

where k_{obs} can be calculated at a given pH using $k_{18} = (8.3 \pm 0.7) \times 10^5\ M^{-1}\ s^{-1}$, $k_{19} = (9.7 \pm 0.6) \times 10^7\ M^{-1}\ s^{-1}$, and $K_{HO_2^{\cdot}} = 1.6 \times 10^{-5}$ M as recommended values.[9] The rate of second-order reaction mainly given by the reactions of 18 and 19 is

$$-\frac{d[HO_2^{\cdot}/O_2^{\cdot-}]}{dt} = k_{obs}[HO_2^{\cdot}/O_2^{\cdot-}]^2 \quad (II)$$

The solution of equation (II) is

$$k_{obs} \times t = \frac{[HO_2^{\cdot}/O_2^{\cdot-}]_o - [HO_2^{\cdot}/O_2^{\cdot-}]_t}{[HO_2^{\cdot}/O_2^{\cdot-}]_o \times [HO_2^{\cdot}/O_2^{\cdot-}]_t} \equiv SR = \frac{A_o - A_t}{A_o A_t} \quad (III)$$

where the signal ratio (SR) can be defined as $(A_o - A_t)/(A_o \times A_t)$ where A_o is signal height of fluorescent OHBA at KTR2 of 0 m and A_t is signal heights at KTR2 of 1, 2, 3, and 4 m, respectively. Since $[HO_2^{\cdot}/O_2^{\cdot-}]_{t1/2}$ is equal to $[HO_2^{\cdot}/O_2^{\cdot-}]_o/2$ at the half-life ($t_{1/2}$), equation (III) becomes

$$[HO_2^{\cdot}/O_2^{\cdot-}]_o = \frac{1}{k_{obs} \times t_{1/2}} \quad (IV)$$

In the case of the second-order reaction, the $t_{1/2}$ is inversely proportional to the initial concentration of $HO_2^{\cdot}/O_2^{\cdot-}$. Thus, the concentration of $HO_2^{\cdot}/O_2^{\cdot-}$ can readily be determined from the $t_{1/2}$ of $HO_2^{\cdot}/O_2^{\cdot-}$ decay in the aqueous solution with calculated k_{obs} at a given pH.

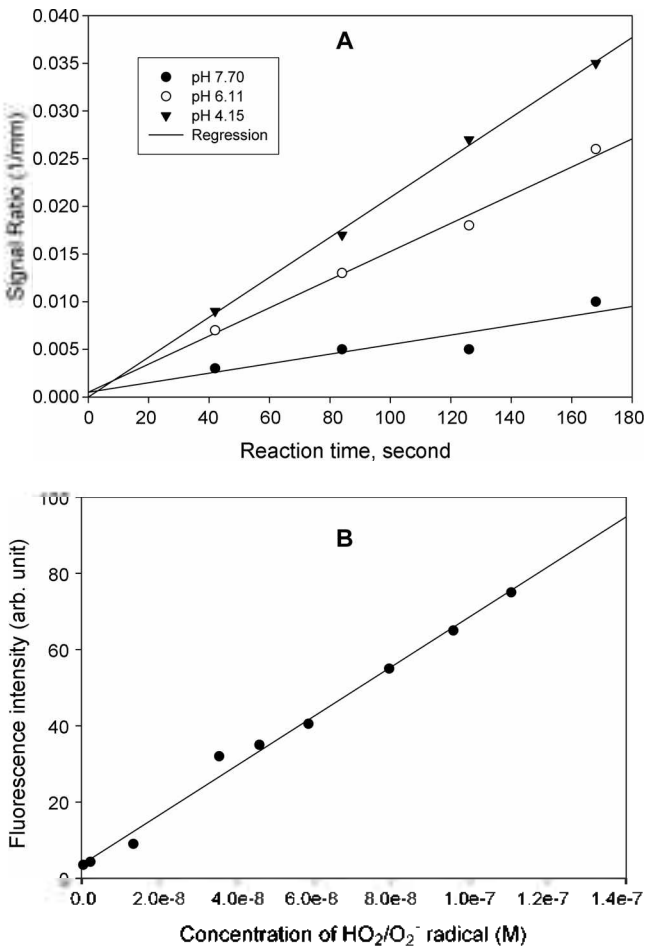

Figure 2. A: Plot of SR vs. reaction time with straight line: [BA] = 1 mM, $[H_2O_2]$ = 4 mM, $[Fe^{3+}$-EDTA] = 20 μM, and [NaOH] = 0.05 N. B: Linear plot of fluorescence signal intensity versus concentration of $HO_2^{\cdot}/O_2^{\cdot-}$: pH = 6.11 and same as A. Figure 2 B is fitted by the least squares method using the SigmaPlot (ver. 8.0).

The half-life ($t_{1/2}$) of $HO_2^{\cdot}/O_2^{\cdot-}$ is experimentally measured with plotting linear relationship of SR *vs.* reaction time based on each length of KTR2. Since self-reactions of 18 and 19 occur in KTR2, the concentrations of $HO_2^{\cdot}/O_2^{\cdot-}$ can be expected to decrease with increasing length of KTR2, which are stepwise varied as 0, 1, 2, 3, and 4 m. Hence the fluorescence intensity of OHBA corresponding to the concentration of $HO_2^{\cdot}/O_2^{\cdot-}$ is decreased with increasing length of KTR2, which is converted into reaction time by the constant flow rate through KTR2 and their constant volumes. A plot of SR *vs.* reaction time gives a straight line (Figure 2a) as expected, which produces a pair of slope and intercept at a given pH. From this slope and intercept, we derived the half-life ($t_{1/2}$) as following equation (V):

$$SR_{t1/2} = \text{Slope} \times t_{1/2} + \text{Intercept} \quad \text{(V)}$$

where $SR_{t1/2}$ is the SR of half-life and becomes identical with $1/A_o$ at $t_{1/2}$. Consequently, a given concentration of $HO_2^{\cdot}/O_2^{\cdot-}$ is kinetically calculated from the equation (IV), based on the measured $t_{1/2}$ and calculated k_{obs} at a given pH. The fluorescence intensity using various irradiation time of H_2O_2 to produce different quantities of $HO_2^{\cdot}/O_2^{\cdot-}$ is linear at pH 6.12 as shown in Figure 2b.

Results and Discussion

Potential interferences and their elimination. As mentioned earlier, $^{\cdot}OH_{(O3)}$ and O_3 are considered as potential interfering oxidants for the use of the kinetic method. The fluorescence intensity of OHBA against various concentrations of O_3 in the absence of Fe^{3+}-EDTA is given in Figure 3, in which the fluorescence signal shows a reasonable response to $^{\cdot}OH_{(O3)}$ and O_3. The possible formation pathways of OHBA may be resulted from the hydroxylation of BA by O_3 (reaction 12) and $^{\cdot}OH_{(O3)}$ (reaction 15). Although the direct hydroxylation of BA by O_3 (k_{12} = 1.2

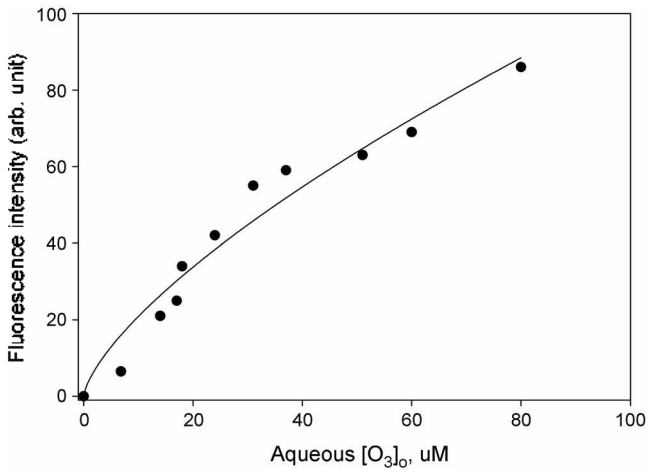

Figure 3. Dependence of the fluorescence intensity on increasing O_3 concentration in the absence of Fe^{3+}-EDTA: pH = 4.9, [BA] = 1 mM, [H_2O_2] = 4 mM, and [NaOH] = 0.05 N. The fitting method is the hyperbola method with nonlinear regression using SigmaPlot (ver. 8.0).

$M^{-1}s^{-1}$) is negligible,[5] O_3 decomposition in water can continuously generate $^{\cdot}OH_{(O3)}$ which reacts very rapidly with BA (k_{15} = 4.3 × 10^9 M^{-1} s^{-1}) to produce OHBA.[15] Thus, $^{\cdot}OH_{(O3)}$ and O_3 have to be eliminated prior to their reactions with Fe^{3+}-EDTA/H_2O_2/BA for $HO_2^{\cdot}/O_2^{\cdot-}$ determination using the kinetic method. This prompted us to seek a proper scavenging compound that would suppress $^{\cdot}OH_{(O3)}$ and O_3 while minimizing the quenching of the fluorescence signal of OHBA generated from $^{\cdot}OH_{(O3)}$.

Several compounds such as formate ($HCOO^-$), alcohols (*i.e.*, methanol and ethanol), nitrite (NO_2^-), and sulfite (SO_3^{2-}) were considered as scavengers for suppressing both $^{\cdot}OH_{(O3)}$ and O_3. Formate, methanol, and ethanol, however, lead to a production of additional $HO_2^{\cdot}/O_2^{\cdot-}$ in the presence of $^{\cdot}OH_{(O3)}$[7] and react very slow with O_3, k = 0.02-100 M^{-1} s^{-1}.[5] In addition, nitrite reacts fast not only with $^{\cdot}OH_{(O3)}$ and O_3 but also with $HO_2^{\cdot}/O_2^{\cdot-}$.[5,9,15] Hence, formate, alcohols, and nitrite are not proper scavengers in the kinetic method for $HO_2^{\cdot}/O_2^{\cdot-}$ determination. On the other hand, it has been well known the chain oxidation mechanism of HSO_3^-/SO_3^{2-} in aqueous solution. As expected from kinetic considerations, HSO_3^-/SO_3^{2-} is considered as a possible scavenger of both $^{\cdot}OH_{(O3)}$ and O_3. The interfering effects of O_3 and $^{\cdot}OH_{(O3)}$ in the kinetic method may be effectively suppressed by addition of HSO_3^-/SO_3^{2-} as follow:[4,5,9,16-20]

$$O_3 + SO_3^{2-} \rightarrow \text{products} \quad (20)$$

$$O_3 + HSO_3^- \rightarrow \text{products} \quad (21)$$

$$^{\cdot}OH_{(O3)} + SO_3^{2-} \rightarrow OH^- + SO_3^{\cdot-} \quad (22)$$

$$^{\cdot}OH_{(O3)} + HSO_3^- \rightarrow H_2O + SO_3^{\cdot-} \quad (23)$$

$$O_2^{\cdot-} + SO_3^{2-} (+ H_2O) \rightarrow SO_3^{\cdot-} + HO_2^- + OH^- \quad (24a)$$

$$HO_2^{\cdot} + HSO_3^- \rightarrow \text{products} \quad (24b)$$

$$HSO_3^- \leftrightarrow SO_3^{2-} + H^+ \quad pK_a = 7.2 \quad (25)$$

where k_{20} = 1.0 × 10^9 M^{-1} s^{-1}, k_{21} = 3.2 × 10^5 M^{-1} s^{-1}, k_{22} = 5.5 × 10^9 M^{-1} s^{-1}, k_{23} = 4.5 × 10^9 M^{-1} s^{-1}, k_{24a} = 82 M^{-1} s^{-1}, and k_{24b} < 20 M^{-1} s^{-1}. O_3 and $^{\cdot}OH_{(O3)}$ react rapidly with HSO_3^-/SO_3^{2-} at nearly diffusion-controlled rate (reactions of 20, 22, and 23), whereas $HO_2^{\cdot}/O_2^{\cdot-}$ reacts very slow with HSO_3^-/SO_3^{2-} (reactions of 24a and 24b). $SO_3^{\cdot-}$ formed in reactions 22-24a would be removed by dissolved O_2 with k_{26} = 1.5 × 10^9 $M^{-1}s^{-1}$:[5]

$$2SO_3^{\cdot-} + O_2 \rightarrow\rightarrow\rightarrow 2SO_4^{2-} \quad (26)$$

In order to examine the scavenging effect of HSO_3^-/SO_3^{2-} on both $^{\cdot}OH_{(O3)}$ and O_3, the kinetic method for $HO_2^{\cdot}/O_2^{\cdot-}$ measurement is evaluated without and with Fe^{3+}-EDTA. In the absence of the Fe^{3+}-EDTA, Figure 4 shows the dependence of the fluorescence intensity of OHBA on HSO_3^-/SO_3^{2-} concentration at various pH conditions of 4.11-8.35. The fluorescence intensity of OHBA is rapidly decreased by gradually increasing HSO_3^-/SO_3^{2-} concentrations in the ranges of 0.001-0.01 mM and is slowly decreased thereafter. It suggests that HSO_3^-/SO_3^{2-} effectively eliminates residual O_3 and $^{\cdot}OH_{(O3)}$ formed by ozone decomposition. After eliminating O_3 and $^{\cdot}OH_{(O3)}$, residual SO_3^{2-} may compete

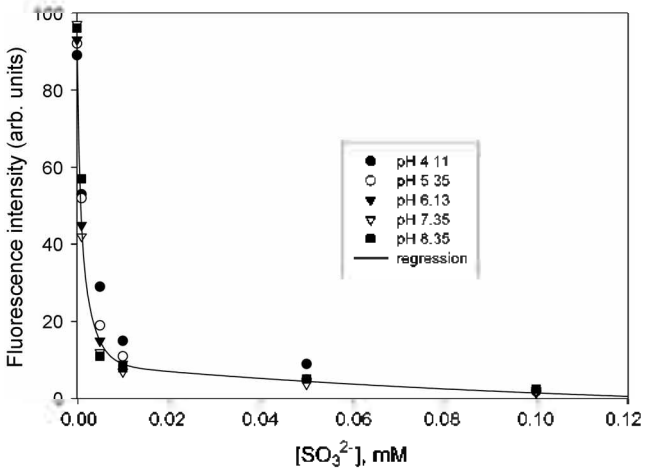

Figure 4. Dependence of the fluorescence intensity on increasing of SO_3^{2-} concentration in the absence of Fe^{3+}-EDTA and in different pH conditions: $[O_3]$ = 60 μM, [BA] = 1 mM, $[H_2O_2]$ = 4 mM, and [NaOH] = 0.05 N. The fitting method is the exponential decay method using SigmaPlot (ver. 8.0).

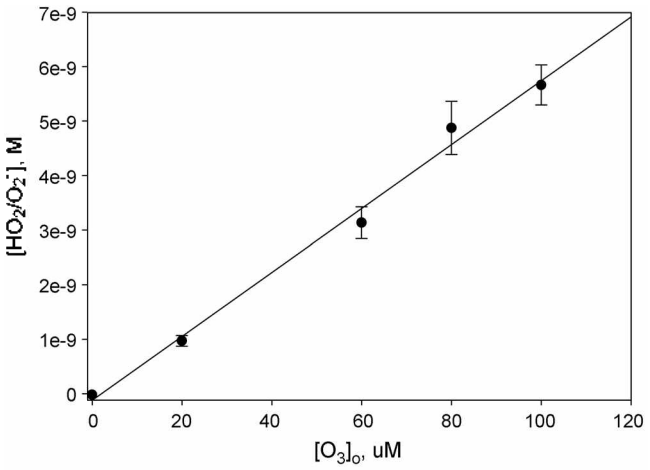

Figure 6. The steady-state concentration of $HO_2^{\cdot}/O_2^{\cdot-}$ depending on initial O_3 concentration: pH = 4.9, $[SO_3^{2-}]$ = 0.1 mM, $[Fe^{3+}$-EDTA] = 20 μM, [BA] = 1 mM, $[H_2O_2]$ = 4 mM, and [NaOH] = 0.05 N. The fitting method is the least squares method using SigmaPlot (ver. 8.0).

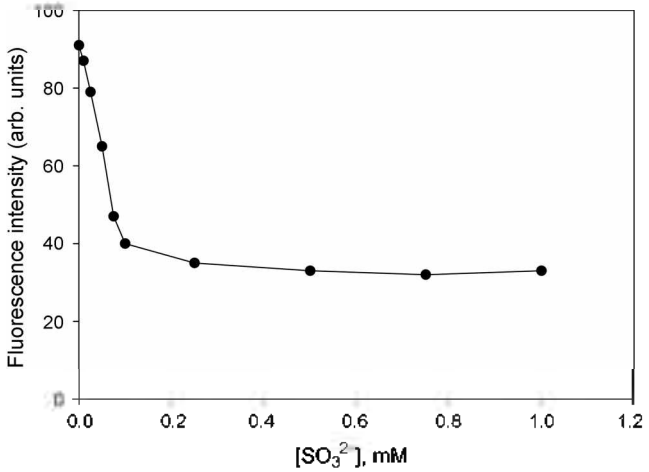

Figure 5. Dependence of the fluorescence intensity on increasing of SO_3^{2-} concentration in the presence of $[Fe^{3+}$-EDTA] = 20 μM: pH = 4.9, $[O_3]$ = 60 μM, [BA] = 1 mM, $[H_2O_2]$ = 4 mM, and [NaOH] = 0.05 N.

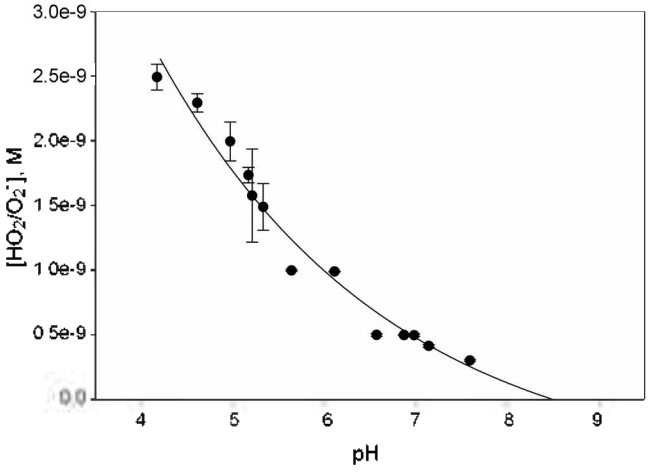

Figure 7. Dependence of the steady-state $HO_2^{\cdot}/O_2^{\cdot-}$ concentrations on pH: $[SO_3^{2-}]$ = 0.1 mM, $[Fe^{3+}$-EDTA] = 20 μM, [BA] = 1 mM, $[O_3]$ = 60 μM, $[H_2O_2]$ = 4 mM, and [NaOH] = 0.05 N. The fitting method is the exponential method using SigmaPlot (ver. 8.0).

with BA for $^{\cdot}OH_{(TL)}$. This competing reaction would be eliminated by the oxidation of residual HSO_3^-/SO_3^{2-} by excess H_2O_2 prior to the Fenton-like reaction. On the other hand, in the presence of Fe^{3+}-EDTA the fluorescence intensity of OHBA is measured at pH 4.9 as shown in Figure 5. The fluorescence intensity of OHBA is rapidly decreased by gradually increasing sulfite concentration in the ranges of 0-0.1 mM and thereafter reaches at a steady fluorescence intensity. This rapid decrease of the fluorescence signal indicates that residual O_3 and $^{\cdot}OH_{(O3)}$ formed by O_3 decomposition are properly eliminated by sulfite, and the steady fluorescence signal of OHBA is caused by $HO_2^{\cdot}/O_2^{\cdot-}$ through the reduction of Fe^{3+}-EDTA into Fe^{2+}-EDTA followed by the Fenton-like reaction of H_2O_2 and Fe^{2+}-EDTA in the presence of BA. These results suggest that the kinetic method using HSO_3^-/SO_3^{2-} can be used to determine the steady-state concentration of $HO_2^{\cdot}/O_2^{\cdot-}$ formed in O_3 decomposition.

Determination of $HO_2^{\cdot}/O_2^{\cdot-}$. The steady-state concentration of $HO_2^{\cdot}/O_2^{\cdot-}$ in aqueous O_3 solution was measured by using the kinetic method as a function of initial O_3 concentration at pH 4.9 using a continuous flow system as shown in Figure 6. The concentration of $HO_2^{\cdot}/O_2^{\cdot-}$ increases with increasing the O_3 concentration, which shows a reasonable linearity within the experimental error. These results suggest that the steady-state $HO_2^{\cdot}/O_2^{\cdot-}$ concentration is proportional to the O_3 concentration at a given pH.

The steady-state concentration of $HO_2^{\cdot}/O_2^{\cdot-}$ generated during O_3 decay shows pH dependence in the range of pH 4-7.59 as shown in Figure 7 and in Table 1, and they are ranging from 2.49 ($\pm$ 0.10) $\times$ 10^{-9} M (pH = 4.17) ~ 3.01 ($\pm$ 0.07) $\times$ 10^{-10} M (pH = 7.59) at $[O_3]_o$ = 60 μM. The pH

Table 1. Dependence of the steady-state $HO_2^{\cdot}/O_2^{\cdot-}$ concentrations on pH

pH	Concentration of $HO_2^{\cdot}/O_2^{\cdot-}$ (±)[a], M
4.17	$2.49 (\pm 0.10) \times 10^{-9}$
4.61	$2.29 (\pm 0.07) \times 10^{-9}$
4.97	$1.99 (\pm 0.15) \times 10^{-9}$
5.17	$1.73 (\pm 0.06) \times 10^{-9}$
5.21	$1.58 (\pm 0.36) \times 10^{-9}$
5.33	$1.49 (\pm 0.18) \times 10^{-9}$
5.64	$9.97 (\pm 0.06) \times 10^{-10}$
6.11	$9.88 (\pm 0.03) \times 10^{-10}$
6.57	$4.98 (\pm 0.11) \times 10^{-10}$
6.87	$4.98 (\pm 0.05) \times 10^{-10}$
6.98	$4.96 (\pm 0.10) \times 10^{-10}$
7.14	$4.14 (\pm 0.10) \times 10^{-10}$
7.59	$3.01 (\pm 0.07) \times 10^{-10}$

[a]the errors in parentheses refer to standard deviation

dependence of $HO_2^{\cdot}/O_2^{\cdot-}$ concentration is distinguished from the different reactivities of $HO_2^{\cdot}$ and $O_2^{\cdot-}$ on O_3 molecules. Based on pK_a ($HO_2^{\cdot}$) = 4.8, at low pH condition $[HO_2^{\cdot}]/[O_2^{\cdot-}]$ ratio is high and $HO_2^{\cdot}$ reacts very slow with O_3 ($k_7 < 10^4\ M^{-1}s^{-1}$).[21] Thus, the steady-state concentration of $HO_2^{\cdot}$ is relatively high. On the other hand, as the pH increases, $[HO_2^{\cdot}]/[O_2^{\cdot-}]$ ratio rapidly decreases. Since the reaction between $O_2^{\cdot-}$ and O_3 ($k_6 = 1.52 (\pm 0.05) \times 10^9\ M^{-1}s^{-1}$)[2,11] is very fast, the loss rate of $O_2^{\cdot-}$ by O_3 is increased as pH increases. Thus, its concentration obtained by the kinetic method is relatively low or even undetectable at higher pH (> 8).

However, any quantitative concentration of $HO_2^{\cdot}/O_2^{\cdot-}$ measured in the ozone decomposition in water has not been found from a number of previous studies. Staehelin *et al.*[7] reported without specifying pH condition that the steady-state concentration of $HO_2^{\cdot}/O_2^{\cdot-}$ was estimated to be $\leq 10^{-9}$ M, assuming that formation rate of $HO_2^{\cdot}/O_2^{\cdot-}$ is $\leq 10^{-5}$ M/s and ozone concentration of $\leq 10^{-5}$ M controls its consumption rate. It is fortuitous that the steady-state concentrations of $HO_2^{\cdot}/O_2^{\cdot-}$ measured in this study find a reasonable agreement with their results.

Conclusions

The concentration of $HO_2^{\cdot}/O_2^{\cdot-}$ in ozone decomposition has been determined by the novel kinetic method using the experimentally determined half-life ($t_{1/2}$). $HO_2^{\cdot}/O_2^{\cdot-}$ formed in ozone decomposition reduce Fe^{3+}-EDTA into Fe^{2+}-EDTA and subsequently the well-known Fenton-like (FL) reaction of H_2O_2 and Fe^{2+}-EDTA produces the hydroxyl radicals, $^{\cdot}OH_{(FL)}$. Benzoic acid (BA) scavenges $^{\cdot}OH_{(FL)}$ to produce OHBA, which are analyzed by fluorescence detection (λ_{ex} = 320 nm and λ_{em} = 400 nm). In this study, potential interferences of O_3 and the hydroxyl radicals, $^{\cdot}OH_{(O3)}$, are suppressed by HSO_3^-/SO_3^{2-}. The steady-state concentration of $HO_2^{\cdot}/O_2^{\cdot-}$ is proportional to the O_3 concentration at a given pH. However, the steady-state concentration of $HO_2^{\cdot}/O_2^{\cdot-}$ in ozone decomposition is inversely proportional to pH values. This pH dependence is due to significant loss of $O_2^{\cdot-}$ by O_3 at high pH conditions. The steady-state concentrations of $HO_2^{\cdot}/O_2^{\cdot-}$ are in the range of $2.49 (\pm 0.10) \times 10^{-9}$ M (pH = 4.17) ~ $3.01 (\pm 0.07) \times 10^{-10}$ M (pH = 7.59) at $[O_3]_o = 60\ \mu M$.

Acknowledgements. This work was supported by Ministry of Environment as "the Eco-technopia 21 project" and in part by the Korea Science and Engineering Foundation (KOSEF) through the Advanced Environmental Monitoring Research Center (ADEMRC) at Gwangju Institute of Science and Technology (GIST) and the Brain Korea 21 Project, Ministry of Education and Human Resources Development Korea.

References

1. von Gunten, U. *Wat. Res.* **2003**, *37*, 1443-1467.
2. Bühler, R. E.; Staehelin, J.; Hoigne, J. *J. Phys. Chem.* **1984**, *88*, 2560-2564.
3. Hoigne, J.; Bader, H. *Wat. Res.* **1976**, *10*, 377-386.
4. Hoigne, J.; Bader, H.; Haag, W. R.; Staehelin, J. *Wat. Res.* **1985**, *19*, 993-1004.
5. Neta, P.; Huie, R. E.; Ross, A. B. *J. Phys. Chem. Ref. Data* **1988**, 17.
6. Staehelin, J.; Hoigne, J. *Environ. Sci. Technol.* **1982**, *16*, 676-681.
7. Staehelin, J.; Hoigne, J. *Environ. Sci. Technol.* **1985**, *19*, 1206-1213.
8. Flyunt, R.; Leitzke, A.; Mark, G.; Mvula, E.; Reisz, E.; Schick, R.; von Sonntag, C. *J. Phys. Chem B* **2003**, *107*, 7242-7253.
9. Bielski, B. H. J.; Cabelli, D. E.; Arudi, R. L.; Ross, A. B. *J. Phys. Chem. Ref. Data* **1985**, 14.
10. Forni, L.; Bahnemann, D.; Hart, E. J. *J. Phys. Chem.* **1982**, *86*, 255-259.
11. Sehested, K.; Holcman, J.; Hart, E. J. *J. Phys. Chem.* **1983**, *87*, 1951-1954.
12. Kwon, B. G.; Lee, J. H. *Anal. Chem.* **2004**, *76*, 6359-6364.
13. Bader, H.; Hoigne, J. *Wat. Res.* **1981**, *9*, 449-456.
14. Bull, C.; McClune, G. J.; Fee, J. A. *J. Am. Chem. Soc.* **1983**, *105*, 5290-5300.
15. Buxton, G. V.; Greenstock, C. L.; Helman, W. P.; Ross, A. B. *J. Phys. Chem. Ref. Data* **1988**, 17.
16. Sadat-Shafai, T.; Pucheault, J.; Ferradini, C. *Radiat. Phys. Chem.* **1981**, *17*, 283-288.
17. Hayon, E.; Treinin, A.; Will, J. *J. Phys. Chem.* **1972**, *94*, 47-57.
18. Fischer, M.; Warneck, P. *J. Phys. Chem.* **1996**, *100*, 15111-15117.
19. Das, T. N.; Huie, R. E.; Neta, P. *J. Phys. Chem. A* **1999**, *103*, 3581-3588.
20. Yermakov, A. N.; Zhitomirsky, B. M.; Poskrebyshev, G. A.; Stoliarov, S. I. *J. Phys. Chem.* **1995**, *99*, 3120-3127.
21. Sehested, K.; Holcman, J.; Bjergbakke, E.; Hart, E. J. *J. Phys. Chem.* **1984**, *88*, 4144-4147.

Appdendix

Estimation for the extinction coefficient of aqueous ozone. Up to now, previous studies are not presenting the extinction coefficient of aqueous ozone for the wavelength range 200 to 240 nm because of the instability of ozone in water. In this study, the extinction coefficient of ozone in water at 220 nm is extrapolating from the cross section of ozone, based on the well-known $\varepsilon_{258nm} = 2{,}900\ M^{-1}cm^{-1}$. The cross sections of gaseous ozone in the atmosphere have a value of $1{,}120 \times 10^{-20}$ cm^2 at 258 nm and 199×10^{-20} cm^2 at 220 nm, respectively. The cross section values of gaseous ozone in the atmosphere can get from NASA, (2003) JPL Publication 02-25, 4-8.